

1 **STRUCTURAL STRENGTHENING WITH**
2 **PRESTRESSED CFRP STRIPS WITH GRADIENT**
3 **ANCHORAGE**

4 Julien Michels¹, Jose Sena-Cruz², Christoph Czaderski³ and Masoud Motavalli⁴, Member, ASCE

5 **ABSTRACT**

6 This paper presents the principle and the application of an innovative anchorage
7 technique for prestressed carbon-fiber reinforced polymer (CFRP) strips in struc-
8 tural strengthening. **Additionally, large-scale static loading tests of retrofitted con-**
9 **crete beams are shown.** The gradient anchorage, based on the adhesive's ability
10 to undergo accelerated curing at high temperatures, consists of a purely concrete-
11 adhesive-strip connection without any mechanical devices such as bolts or plates. In
12 a first step, this study summarizes anchorage techniques presented in the literature

¹PhD, Project Leader, Structural Engineering Research Laboratory, Swiss Federal Laboratories for Materials Science and Technology (Empa), Überlandstrasse 129, CH-8600 Dübendorf, Switzerland. E-mail: julien.michels@empa.ch

²PhD, Associate Professor, ISE, Department of Civil Engineering, University of Minho, 4800-058 Guimarães, Portugal, E-Mail: jsena@civil.uminho.pt

³PhD, Senior Scientist, Structural Engineering Research Laboratory, Swiss Federal Laboratories for Materials Science and Technology (Empa), Überlandstrasse 129, CH-8600 Dübendorf, Switzerland. E-mail: christoph.czaderski@empa.ch

⁴PhD, Assistant Professor, Laboratory Head, Structural Engineering Research Laboratory, Swiss Federal Laboratories for Materials Science and Technology (Empa), Überlandstrasse 129, CH-8600 Dübendorf, Switzerland. E-mail: masoud.motavalli@empa.ch

13 and introduces the basic principles of the new method as well as the necessary com-
14 ponents. In a second step, an application on a full-scale RC beam is explained in
15 detail. A commercially available CFRP strip is prestressed up to 0.6 % prestrain and
16 subsequently anchored by sequential epoxy-curing and force-releasing steps at both
17 strip ends. **Furthermore**, uniaxial tensile tests on the epoxy adhesive and the CFRP
18 strip are used for material characterization and to demonstrate the reinforcing mate-
19 rials' integrity after the heating process. It appeared that prestress losses during the
20 anchoring phase are negligible. Furthermore, the method allows a much faster instal-
21 lation compared to conventional mechanical techniques and increases durability as
22 no permanent steel elements are necessary. The material tests indicate no damage in
23 the reinforcing CFRP strip as well as a sufficiently fast strength development of the
24 adhesive after accelerated curing. Static loading tests on strengthened large-scale RC
25 beams are presented and show the efficiency of a prestressed CFRP strip with gradi-
26 ent anchorage as a retrofitting technique. **Finally, first long-term measurements over**
27 **13 years on a prestressed strip bonded to a concrete plate revealed small prestrain**
28 **losses.**

29 **Keywords:** structural retrofitting, prestressed CFRP strips, epoxy adhesive, accel-
30 erated curing, innovative anchorage technique, gradient anchorage

31 INTRODUCTION

32 Historically, the use of fiber reinforced polymer (FRP) materials for upgrading
33 existing reinforced concrete (RC) structures started in the early 1980s. Since then,
34 tremendous developments occurred during the following decades, this regarding the
35 materials, their application systems as well as the theoretical knowledge for design

36 purposes. The advantages of composite materials in structural retrofitting applica-
37 tions are well documented in the literature ([Bakis et al. 2002](#)). Externally bonded
38 reinforcement (EBR) is the most common flexural strengthening technique with FRP
39 materials. Such reinforcements are glued to the tensile surfaces of the structure to
40 be strengthened. Usually, epoxy adhesives are used as a connector. Among the
41 commercially available FRP, carbon (CFRP) materials are the most spread. Due
42 to their low density, high stiffness, high tensile strength, long fatigue life and less
43 susceptibility to aggressive environments ([CEB-Bulletin-No.235 1997](#)), this type of
44 additional reinforcement has gained increasing popularity.

45 Prestressed FRP for strengthening of RC structures combines the benefits of pas-
46 sive EBR FRP systems with the advantages associated with external prestressing.
47 Over the last two decades prestressed FRPs have been applied and considerable
48 advantages have been pointed out ([Svecova and Razaqpur 2000](#)), ([El-Hacha et al.
49 2001](#)), ([El-Hacha et al. 2003](#)), ([Wight et al. 2001](#)), ([Woo et al. 2008](#)), ([Pellegrino
50 and Modena 2009](#)), ([Motavalli et al. 2011](#)): deflection reduction and acting against
51 dead loads, crack widths reduction, delay in the onset of cracking, strain relief within
52 the internal steel reinforcement, higher fatigue failure resistance, delay in yielding of
53 the internal steel reinforcements, more efficient use of concrete and FRP, reduction of
54 premature debonding failure, increase in ultimate load bearing capacity and increase
55 in shear capacity. Strips, sheets and bars are the most common prestressed FRP
56 shapes, the first ones being the most prominent. Mainly three procedures have been
57 developed to induce prestress in the FRP: cambered prestressing systems ([El-Hacha
58 et al. 2001](#)), prestressing against an independent element ([El-Hacha et al. 2001](#)),

59 (Xue et al. 2010) and prestressing against the element to be strengthened (El-Hacha
60 et al. 2001), (Woo et al. 2008), (Pellegrino and Modena 2009), (Tateishi et al. 2007),
61 (Neubauer et al. 2007), (França and Costa 2007), (El-Hacha et al. 2009). Among
62 these techniques, the latter procedure can be judged the most suitable for practical
63 application. Like non-prestressed systems, structural epoxy adhesives are generally
64 used to bond the FRP element to the concrete substrate.

65

66 At the ends of a prestressed FRP element, special end-anchorage is required in
67 order to transfer the forces from the EBR to the concrete surface and hence to avoid
68 premature peeling-off failure (Triantafillou et al. 1992). Up to now, the proposed
69 end-anchorage systems can be divided in three categories: metallic anchors (Woo
70 et al. 2008), (Pellegrino and Modena 2009), (Xue et al. 2010), (Suter and Jungo
71 2001), (Xue et al. 2008) non-metallic anchors (Kim et al. 2008), (Berset et al. 2002)
72 and the gradient anchorage (Meier and Stöcklin 2005).

73 The latter method consists in gradually reducing the prestressing force at the FRP
74 strip ends towards zero over a predefined length. (Wu et al. 2003) use several layers
75 of FRP sheets for the flexural strengthening and for decreasing the level of stresses at
76 the ends. Each FRP longitudinal sheet, at the ends, is anchored by using U-shaped
77 FRP sheets. The other system, proposed by (Meier and Stöcklin 2005) uses a special
78 stressing and heating device. The prestress force gradient is obtained by sector-wise
79 heating and curing of the adhesive followed by step-wise force releasing in the hy-
80 draulic jack. With such a system, permanent anchorage (e.g., steel plate) is no longer
81 necessary. Up to now the research performed with this method includes the bond

82 behavior analysis at the anchorage region using lap-shear and prestress-force-release
83 tests (Czaderski et al. 2012) as well as large scale structural tests on retrofitted RC
84 elements. In full-scale tests with prestressed bridge girders with 17 m span (Czaderski
85 and Motavalli 2007), a load increase in ultimate bearing capacity of 45% of the cor-
86 responding control structural element and 17.5 % compared to an unstressed CFRP
87 strip reinforcement was noticed. In some cases the CFRP strip even reached its ul-
88 timate tensile strength (Meier and Stöcklin 2005), (Kotynia et al. 2011). Long-term
89 bond performance on mechanically anchored prestressed FRP strips was studied for
90 example by Diab et al. (Diab et al. 2009). Additionally, fatigue tests at high temper-
91 atures with gradient anchorage were judged satisfying (Kotynia et al. 2011), failure
92 finally always occurred by internal steel rupture. In a recently completed research
93 and development project a suitable device for practical application on construction
94 site has been developed for the industry (Michels et al. 2012a). Additionally, a the-
95 oretical and experimental investigation was performed in order to study the effect of
96 a prestress force release on the anchorage pulling resistance (Czaderski 2012). This
97 paper presents the method's characteristics, the different necessary components and
98 measurements during a beam retrofitting application. Additionally, tensile tests on
99 both the CFRP strip and the epoxy adhesive after different stress and heating ex-
100 posure were performed in order to demonstrate the reinforcing materials' integrity
101 after the heating process. Lastly, structural performance is demonstrated by a series
102 of large-scale static loading tests on strengthened RC beams. A first impression on
103 long-term behavior is given by presenting results of several strain measurements in
104 time (13 years) on a prestressed strip used for retrofitting of a concrete plate.

105 GRADIENT ANCHORAGE

106 Principle

107 The gradient anchorage is based on the adhesive's ability to cure faster at high
108 temperatures (Michels et al. 2012b). This accelerated curing property is used to
109 create a non-mechanical anchorage purely composed of the CFRP strip, the concrete
110 surface and the intermediate adhesive layer. The principle is a segment-wise heating
111 and force releasing at the strip end, consequently distributing the total prestress force
112 over several gradient segments and hence avoiding a premature debonding failure.
113 Such a failure might occur in case a too high prestress force would be released in
114 one step (Triantafillou et al. 1992). A schematic representation of the anchorage
115 technique is given in Figure 1. After a first adhesive segment 1 with a length Δl_1
116 has been cured at high temperature for a defined duration, its strength has suffi-
117 ciently developed to carry a portion ΔF_1 of the total prestress force F_p , which will
118 subsequently be released. At this stage, the remaining force in the hydraulic jack is
119 $F_p - \Delta F_1$. This procedure is repeated until zero prestress force remains at the strip
120 end. A qualitative force transfer is shown in Figure 2. In case of n accelerated
121 curing/releasing steps, the respective force in the jack at the i^{th} stage is:

$$F_{jack,i} = F_p - \sum_{i=1}^n \Delta F_i \quad (1)$$

122 This procedure is evidently followed simultaneously at both strips end. The force
123 in the strip over the free length outside the anchorage area remains theoretically
124 constant at F_p .

125 **Necessary components and installation procedure**

126 A photo of the different components is given in Figure 3. The total device is
127 composed of the following elements: a) base angles, b) clamps, c) aluminum frame,
128 d) manometer, e) hydraulic jack and f) electronic heating device.

129 The installation procedure is schematically presented in Figure 4. The following
130 steps have to be executed:

- 131 • drilling of the temporary anchor bolts a)
- 132 • placement of the base angles and the clamps rigidly in the exact position a)
- 133 • placement of the CFRP strip (after having spread the epoxy adhesive) a) and
134 closing the clamps with a dynamometric key b)
- 135 • fixing of the electronic heating device b)
- 136 • fixing of the aluminum frame c)
- 137 • installation of the hydraulic jack d)
- 138 • loosening of the base plates in order to allow a smooth sliding of the clamp
139 during the prestressing and force releasing

140 After having installed the different components, the prestressing phase can start.
141 The hydraulic jacks are used simultaneously at both strip ends to deliver the neces-
142 sary force for the strip elongation. The force should be slowly increased up to the
143 desired prestrain. For the presented laboratory application, which is presented in
144 the following section, two strain gauges were used to electronically follow the rise in
145 strain during the prestress phase. For a construction site application, strain is gener-
146 ally checked by visual **control** and measuring the length increase on predefined marks

147 on the strip and concrete surface **or by applying strain gauges to the CFRP**. When
148 the desired prestrain is reached, the valves are closed and the heating of the first
149 segment on both sides starts, lasting for a defined time span. Subsequently, a first
150 force fraction ΔF_1 is released by opening the valves and introduced in the concrete
151 substrate via the cured epoxy adhesive segment. This procedure is repeated until the
152 total prestress force has been completely anchored in the gradient area. The strip is
153 finally cut at both ends, the components can be removed and the temporary anchor
154 bolts can be cut.

155 **Example of beam prestressing**

156 In the present section a strengthening application on a large-scale RC beam
157 (Beam No. 4, see 'Large scale beam tests') with a total length L of 6.5 m and a
158 cross section $b \cdot h$ of 1000 x 220 mm (Figure 5) is presented. Inner steel reinforcement
159 ratio ρ_L was about 0.16 %. 28-days concrete compressive strength on cube $f_{cm,28days}$
160 was 54.1 MPa. The retrofitting is intended to act against positive bending moments
161 between the supports. The strip cross section was $100 \cdot 1.2$ mm ($b_f \cdot t_f$), uniaxial
162 tensile strength $f_{f,u}$ was 2'544 MPa and elastic modulus E_f was 157.8 GPa according
163 to the producer's data sheet ([S&P-Clever-Reinforcement-Company-AG 2011](#)). For
164 simplicity reasons, this laboratory retrofitting application was performed from the
165 top with the plate being turned by 180° along its longitudinal axis as shown in Figure
166 6. With a chosen prestrain $\varepsilon_{f,p}$ of 0.6 %, the force F_p in the laminate corresponds to
167 approximately 120 kN. This stress level of about 1'000 MPa corresponds to 40 % of
168 the ultimate tensile strength $f_{f,u}$. According to previous experimental investigations
169 by the authors ([Michels et al. 2012b](#)), a total heating duration t_h of 25 minutes

170 of accelerated curing at approximately 90°C adhesive temperature and a following
171 cooling duration t_{cool} of about 10 minutes represent an optimum for the used epoxy
172 resin in terms of anchorage capacity. Results have shown that bond lengths l_b of 200
173 and 300 mm with the indicated CFRP strip cross section allow to anchor a maximum
174 force of about 50 and 65 kN, respectively (Michels et al. 2012b). In order to dispose
175 of a sufficient safety when partially releasing the prestress force after accelerated cur-
176 ing, release levels ΔF of 35 and 50 kN were chosen for the mentioned bond lengths.
177 The different releasing steps in relation to the heating device are shown in Figure 7.
178 In total, F_p was released in three steps over a total length of 700 mm, i.e. a first
179 force reduction ΔF_1 of 50 kN over 300 mm (heating elements 1,2 and 3), followed
180 by two consecutive steps ΔF_2 and ΔF_3 of 35 kN over each time 200 mm (heating
181 elements 4,5 and 6,7, respectively). Finally, the epoxy adhesive undergoes acceler-
182 ated curing over a last segment of 100 mm length (heating element 8) without any
183 remaining prestress force in the jack. This last step is used as a supplementary safety
184 against premature debonding. Additionally to the force (oil pressure) measurement
185 in the hydraulic jack as well as the temperature measurement in the heating ele-
186 ments, temperature in the adhesive layer ($T_{a,1}$ to $T_{a,6}$) in the gradient region was
187 followed by means of thermocouples, whose positions are also indicated in Figure 7.
188 As mentioned earlier, a total cooling duration t_{cool} of 10 minutes was introduced af-
189 ter each accelerated curing step in order to let the adhesive temperature drop under
190 the glass transition temperature ($T_g \approx 55^\circ\text{C}$ in this case) before proceeding with the
191 force release. In order to further shorten the total application duration, the heating
192 procedure of the subsequent gradient segment is started during the ongoing cooling

193 duration (overlapping of approximately 5 minutes).

194 In Figure 8, the different characteristic measurements for one anchorage are plotted
195 over time t . In Figure 8 a), prestressing is visible by a rising force in the hydraulic
196 jack. Simultaneously, strain measurements by two gauges (SG1 and SG4, see Fig-
197 ure 14) are presented on a second ordinate axis, eventually presenting a prestrain of
198 about 0.6 % (6000 $\mu m/m$). As soon as the desired force in the jack (and strain in
199 the CFRP strip) is reached, the heating procedure is launched. This is observed by
200 a temperature increase in the heating elements ($T_{h,i}$, Figure 8 b)), almost instantana-
201 nously followed by a temperature rise inside the adhesive ($T_{a,j}$, Figure 8 b)). The
202 target values for the temperatures inside the epoxy adhesive $T_{a,k}$ as well as the nec-
203 essary heating temperature obtained from the heating elements $T_{h,i}$ are explained in
204 detail in (Michels et al. 2012b). In order to increase the temperature in the adhesives
205 as fast as possible, the heating elements had to be configured with an "overheating"
206 temperature. The exact configuration with an initial plateau of 160°C for a time span
207 of 10 minutes followed by an exponential decreasing temperature for 15 minutes de-
208 rives from an extensive study also documented in the previous reference. After the
209 cooling duration, as it can be seen in Figure 8, the jack force is decreased from 120
210 to 75 kN ($\Delta F_1=50$ kN over a bond length of 300 mm), while the prestrain over the
211 free length outside the anchorage regions remains constant (Figure 8 a)). Only a
212 minor slip during the first force release resulting in a prestrain loss $\Delta\varepsilon_{f,p}$ of less than
213 0.01 % is noticed. The total prestress force is afterwards completely reduced to 0 kN
214 by two additional gradient segments of each time 200 mm with 35 kN shear force
215 (ΔF_2 and ΔF_3). At the end, all components will be removed and the temporary

216 anchor bolts are cut. To summarize, a total duration of 130 minutes is necessary
217 to anchor the prestressed CFRP strip. Together with the required preparation work
218 (installation of the bolts, grinding,), a total application duration of about 4 hours
219 can be estimated. Compared to conventional mechanical anchorage systems, which
220 usually require a curing duration at room temperature for the adhesive layer of about
221 1-2 days, the application of the newly developed device is clearly faster and might
222 be economically more attractive.

223 In Figure 9, the evolution of the prestrain in the strip for the first 23 days at room
224 temperature is presented. It gets obvious that no decrease in the CFRP strain has
225 occurred, proof of a stable anchorage at the beam end. The slight enhancement
226 after 500 hours is due to the installation of the beam into the test setup for static
227 loading. After the initial installation of the strip on top of the beam, the latter is
228 again moved to its original position (turned by 180°) with the retrofitting strip on
229 the bottom side. Dead load now acts the opposite way than during the anchorage
230 phase and thus increases the strain in the strip.

231 **EXPERIMENTAL INVESTIGATION**

232 **Bond characteristics**

233 Recent research at Empa has focused both on the development of a suitable device
234 for practical on-site application as well as on the optimization of the heating and
235 releasing procedure in terms of anchorage length and heating duration ([Michels et al.
236 2012b](#)). A large experimental investigation series of pull-off and prestress/release
237 tests with different laminate thickness ([Czaderski et al. 2012](#)), ([Michels et al. 2012b](#))
238 have indicated that after short term curing between 20 and 60 minutes under high

239 temperatures, the epoxy adhesive has gained sufficient (tensile and shear) strength
240 carrying loading forces high enough to provoke debonding failure in the concrete
241 substrate. Compared to specimens cured for 2 to 3 days under room temperature,
242 accelerated curing at high temperatures (approximately 90°C adhesive temperature)
243 evoked higher anchorage resistances, indicating more distributed shear stresses over
244 the bond lengths. This behavior might be due to a lower elastic modulus after
245 the short-term curing process compared to a stiffer material behavior after a longer
246 curing period at room temperature. **The cited references demonstrate that a lower**
247 **elastic modulus of the epoxy involves a higher active bond length and thus higher**
248 **anchorage resistances, due to the low tensile resistance of concrete.** In this paper, the
249 stated characteristics about the epoxy adhesive's elastic modulus are experimentally
250 verified and presented in the upcoming sections. A possible temperature influence
251 on the tensile characteristics of the CFRP strip is investigated, too.

252 **Tensile tests**

253 This section presents experimental analysis on both the epoxy adhesive and the
254 CFRP strip. The first part describes uni-directional tensile tests performed on epoxy
255 resin specimens cured at room temperature for 3 days and cured at high temperature
256 during a short time span, respectively. In the second part, CFRP strip specimens
257 after different heating and stressing treatment were submitted to uniaxial tension in
258 order to assess a possible strength reduction during the anchorage procedure. The
259 goal of the investigation is the assessment of the materials' mechanical performance
260 (stiffness and tensile strength) during the gradient application conditions.

261 The tensile properties of the CFRP strip with a thickness t_f of 1.2 mm were

262 evaluated according to the ISO 527-5:1997(E) ([ISO-527-5](#)) standard. The following
263 configurations were analyzed: unstressed (CFRP-REF), prestressed (CFRP-PRE)
264 and prestressed/heated (CFRP-PH). Prestressed means applying a strain of 0.6 %,
265 identical to the prestress level used for the gradient anchorage. The heating pro-
266 cedure also follows exactly the configuration from the gradient method presented
267 earlier in Figure 8. Temperature $T_{h,i}$ for the heating elements evolves from an initial
268 value of 160°C for 10 minutes followed by an exponential decrease to 120°C during
269 15 minutes. In addition to the investigation of the mechanical properties, physical
270 properties of the distinct series were assessed by visual inspectional and by SEM
271 (Scanning Electron Microscope). Each series was composed of 6 specimens for which
272 the geometry is included in Figure 10. A servo-controlled testing machine was used
273 to perform the tests under a displacement rate of 2 mm/min and a clip gauge with a
274 measuring length of 50 mm was mounted at the middle of each specimen for evaluat-
275 ing the tensile strain. The applied force was recorded by a load cell with a maximum
276 capacity of 200 kN. Prior to the tensile tests, the geometry of all the specimens
277 was assessed by using a digital caliper at 3 specific locations, namely at the spec-
278 imen middle and at 25 mm distance on both sides (top and bottom). Eventually,
279 elastic modulus and tensile strength evaluation was performed by defining a theo-
280 retical cross-section with the average width and thickness dimensions resulting from
281 the three performed measurements. Visual inspection did not reveal any difference
282 between the stressed and heated specimens compared to the reference strips. SEM
283 observations of the strips' cross sections for the series CFRP-REF, CFRP-PRE and
284 CFRP-PH (one for each series) are shown in Figure 11 a), b) and c), respectively.

285 No clear differences were found in these scanning electron microscope observations.
286 Apparently the density of carbon fibers is slightly higher for the CFRP-PRE and
287 CFRP-PH specimens than for the reference strip. This marginal variation was found
288 to be about 8 % and 6 %, respectively, a finding that can be justified with the
289 eventual straightening caused by the prestressing. The tensile test results are sum-
290 marized in Table 1. Negligible variation on the physical and mechanical properties
291 was observed, allowing to say that the adopted procedure for the gradient anchorage
292 application does not affect the overall mechanical behavior of the CFRP strip.

293 For the epoxy adhesive, two configurations are analyzed. For the first category,
294 the formwork with the mixture is kept under constant room temperature (22°C) in
295 a climate chamber for 3 days prior to testing. The second category is subjected to
296 accelerated curing at approximately 90°C (adhesive temperature T_a , see Figure 8)
297 for 25 minutes, followed by a cooling duration of about 10 minutes before the tensile
298 test. The configuration for temperature evolution $T_{h,i}$ of the heating elements was
299 also kept identical to the one used for the beam application presented in Figure 8.
300 Heating is applied by means of the same heating box (Figure 3 and 4) that has also
301 been used for the anchorage application. In this case, the heating device was put on
302 top of the formwork in which the adhesive mixture has been previously introduced.

303 In order to simulate the exact situation as during the prestressing procedure, a piece
304 of CFRP strip was introduced between formwork and heating device, a film was
305 additionally placed between strip and adhesive in order to avoid chemical adhesion.

306 The epoxy resin is a thixotropic, grey two-component mixture, which is commercial-
307 ized by S&P Clever Reinforcement Company under the trademark S&P Resin 220

308 epoxy adhesive ([S&P-Clever-Reinforcement-Company-AG 2012](#)) with the character-
309 istics summarized in Table 2. ISO 527-2:2012(E) standard ([ISO-527-2](#)) was followed
310 in order to evaluate the tensile properties. A servo-controlled testing machine was
311 used to perform the tests under a displacement rate of 1 mm/min. A clip gauge
312 of 50 mm of length was mounted at the middle of each specimen for evaluating the
313 modulus of elasticity (Figure 12). The applied force was measured by means of a
314 load cell with 20 kN of maximum capacity.

315 Prior to the tensile tests, the geometry of all the specimens was assessed using a
316 digital caliper. Three measurements were done along the gauge length, namely, the
317 thickness t and width b , at the top, middle and bottom part of the specimen (bottom
318 and top part being distanced from the middle part by 25 mm). The three values were
319 grouped into an average thickness and width in order to assess an elastic modulus E_f .
320 According to the ISO 527-2 ([ISO-527-2](#)), the elastic modulus shall be determined
321 between strain values of $\varepsilon_1=0.00005$ and $\varepsilon_2=0.00025$. Since not all the specimens
322 reached the level of strain of 0.00025, a second approach was adopted in order to
323 compare the performance of all the series. A maximum strain $\varepsilon_2=0.0015$ was used.
324 This level was selected as the minimum value reached by all the specimens considered
325 in the present analysis. Figure 13 shows stress-strain curves and Table 3 summarizes
326 the results for both the tensile strength and the elastic modulus for the two different
327 curing conditions. It gets obvious that the elastic modulus is clearly lower after a
328 short-term curing process at high temperature compared to the reference specimens
329 cured at room temperature for 3 days. This confirms the assumptions presented in
330 'Bond characteristics', stating that a lower elastic modulus exists for the 25 minutes

331 heating at 90°C. Tensile strength after short-term curing is lower, too. However,
332 with the heating configuration as presented in Figure 8, this characteristic is in the
333 present case not of high importance as the concrete substrate represents the weakest
334 link in the system (Czaderski et al. 2012), (Michels et al. 2012b).

335 **Large scale beam tests**

336 This section summarizes the static loading tests of four strengthened RC beams
337 with gradient anchorage, among them Beam No. 4 presented under 'Example of
338 Beam Prestressing'. The main objective of this section is the demonstration of the
339 gradient anchorage's efficiency. The test setup is shown in Figure 14. The beam was
340 simply supported with a total span of 6 m and subjected to 6-point loading. Average
341 concrete compressive strength on cube at 28 days as well as on the testing day
342 (strength value for Beam 4 was estimated according to (fib bulletin1) as no test result
343 was available) and exact prestrain levels $\varepsilon_{f,p}$ in the CFRP strip for strengthening are
344 listed in Table 4. Equal point loads were applied every 1.2 m under controlled
345 displacement (3 mm/min) at midspan. Deflection at midspan was measured by two
346 displacement transducers, the forces recorded with load cells. Two strain gauges
347 (SG1 and SG4) were mounted on the CFRP strip prior to strengthening in order
348 to assess tensile strain during the prestressing procedure (see 'Example of beam
349 prestressing'). Additional four strain gauges (SG2, SG3, SG5 and SG6) were installed
350 after strengthening. Location of the measurement points is also given in Figure 14.

351 The total force-midspan deflection ($4 \cdot F, w$) diagram of the loading test for all the
352 beams is given in Figure 15. Due to a technical issue no forces were saved for Beam
353 1 during the loading process. Final bearing load of this member was approximately

354 $4 \cdot F_u = 80$ kN. For comparison purposes, a strengthened beam is calculated by means
355 of a simple cross section analysis (CSA) under the assumption of tensile failure of the
356 CFRP strip at 1.6 % tensile strain (S&P-Clever-Reinforcement-Company-AG 2011).
357 Furthermore, the calculated curve of a reference beam with the same cross section
358 but without any additional external reinforcement is displayed. A first beneficial
359 effect is the clear enhancement of the total cracking load $4 \cdot F_{cr}$. For the four beams,
360 the ultimate load occurs clearly after steel yielding. The total bearing load ($4 \cdot F_u$),
361 deflection at failure and maximum CFRP tensile strain at failure are summarized
362 in Table 4. It is visible that for all specimens the failure load is reached before the
363 CFRP strip is able to develop its full tensile strength. Tensile strain increase $\Delta \varepsilon_f$
364 in the CFRP strip up to failure in the range of 0.57 to 0.83 % can be noticed. For
365 Beams 1 and 3 ultimate failure strain was almost attained. Maximum forces $4 \cdot F_u$ are
366 in the current case strongly increased from 16.6 kN for the reference case to values
367 above 65 kN (>290 %).

368 **Long-term behavior**

369 (Stöcklin and Meier 2001) presented strain measurements along the length of a
370 2.4 m long prestressed CFRP strip with gradient anchorage applied in the year 2000
371 on a concrete slab. In the middle part of the strip over approximately a length of 0.8
372 m the strain is more or less constant. A mean prestrain of 0.55% was measured in
373 this area. The slab was stored in the laboratory since then. Figure 16 shows actual
374 photos of the test sample with the prestressed CFRP strip and results of long-term
375 measurements. It can be seen that after almost 13 years the mean prestrain reduced
376 only slightly from 0.55 to 0.51%, most likely due to creep of concrete.

377 CONCLUSIONS

378 The presented R&D activities allow to draw a certain number of conclusions.
379 In the framework of an industry-based project, an efficient heating device has been
380 developed to complete the existing prestressing system. First advantage of the new
381 tool is its easy handling on site. Each component of the total system can be carried
382 by one single person, hence reducing person costs by avoiding a large number of
383 necessary participants. Due to the absence of remaining metallic components such
384 as bolts or plates, the anchorage has a more appealing appearance under service and
385 durability is improved, too. A further positive aspect is the short application time.
386 Including all preparation as well as dismantling steps, the total necessary time span
387 is about 4 hours. Compared to conventional mechanical solutions available on the
388 market, generally requiring 1-2 days of epoxy curing at room temperature before the
389 anchorage is ready for use, the new system is clearly faster. All the above mentioned
390 positive points make the system attractive for future applications. Material testing
391 have shown that the CFRP strip remains undamaged during the heating process,
392 post-heating tensile strength is identical to the reference values. Shortly after the
393 accelerated curing, the epoxy adhesive is softer than the room temperature cured
394 equivalence. However, the temporarily reduced elastic modulus is of advantage for
395 the current application, as earlier research by the authors has proven. Due to
396 the lower stiffness, an attenuation of the shear stresses in the gradient region is
397 registered. The lower tensile strength after short-term heating is of no importance,
398 as the curing of the adhesive has sufficiently advanced for carrying shear stress. Short-
399 term static loading on four retrofitted large-scale beams have shown the efficiency

400 of such a prestressed CFRP strip as additional reinforcement. Both cracking and
401 ultimate loads were significantly increased. **A first long-term analysis of the gradient**
402 **anchorage behavior in time has shown satisfying results with only minimal strain**
403 **losses.**

404 **ACKNOWLEDGEMENTS**

405 The authors want to thank the Swiss innovation promotion agency (CTI project
406 No. 10493.2 PFIW-IW) as well as the industrial partner S&P Clever Reinforcement
407 from Switzerland for their financial support. Furthermore, the staff of the Structural
408 Engineering Testing Laboratory at Empa as well as from University of Minho is
409 kindly thanked for their contributions to the experimental investigations. Particular
410 acknowledgements are expressed to Milos Dimic for the CAD Inventor drawings as
411 well as Professor Fernando Castro from the Department of Mechanical Engineering of
412 the University of Minho for the SEM images. The second author would like to thank
413 the Fundação para a Ciência Fundao para a Cincia e a Tecnologia (Foundation for
414 the Science and Technology/Portugal), grant SFRH/BSAB/1220/2011 for providing
415 financial support in the context of his sabbatical year.

416 **REFERENCES**

- 417 Bakis, C., Bank, L., Brown, V., Cosenza, E., Davalos, J., Lesko, J., Machida, A.,
418 Rizkalla, S., and Triantafillou, T. (2002). “Fiber-reinforced Polymer Composites
419 for Construction - State-of-the-art Review.” *Journal of Composites for Construc-*
420 *tion*, 6(2), 73–87.
- 421 Berset, T., Schwegler, G., and Trausch, L. (2002). “Verstärkung einer Auto-
422 bahnbrücke mit vorgespannten CFK-Lamellen.” *tec21*, 128(22), 22–29.

423 CEB-Bulletin-No.235 (1997). *Serviceability Models - Behaviour and Modelling in Ser-*
424 *viceability Limit States including repeated and sustained loads.* International Fed-
425 eration for Structural Concrete (fib).

426 Czaderski, C. (2012). *Strengthening of Reinforced Concrete Members by Prestressed*
427 *Externally Bonded Reinforcement with Gradient Method.* PhD thesis No. 20504,
428 ETH Zürich, 459 pages, <http://dx.doi.org/10.3929/ethz-a-007569614>.

429 Czaderski, C., Martinelli, E., Michels, J., and Motavalli, M. (2012). “Effect of Curing
430 Conditions on Strength Development in an Epoxy Resin for Structural Strength-

431 ening.” *Composites Part B: Engineering*, 43(2), 398–410.

432 Czaderski, C. and Motavalli, M. (2007). “40-Year-old Full-Scale Concrete Bridge
433 Girder Strengthened with prestressed CFRP Plates anchored using Gradient
434 Method.” *Composites Part B: Engineering*, 38(7-8), 878–886.

435 Diab, H., Wu, Z., and Iwashita, K. (2009). “Short and long-term bond performance
436 of prestressed FRP sheet anchorages.” *Engineering Structures*, 31, 1241–1249.

437 El-Hacha, R., Green, M., and Wight, R. (2009). “Strengthening Concrete Structures
438 with prestressed FRP systems.” *4th International Conference on Construction*
439 *Materials (CONMAT)*, Nagoya, Japan.

440 El-Hacha, R., Wight, R., and Green, M. (2001). “Prestressed Fibre-Reinforced Poly-
441 mer Laminates for Strengthening Structures.” *Progress in Structural Engineering*
442 *and Materials*, 3, 111–121.

443 El-Hacha, R., Wight, R., and Green, M. (2003). “Innovative System for Prestressing
444 Fiber-Reinforced Polymer Sheets.” *ACI Structural Journal*, 100(3), 305–313.

445 fib bulletin1. *Structural Concrete - Textbook on Behaviour, Design and Performance*

446 (Updated knowledge of the CEB/FIP Model Code 1990).

447 França, P. and Costa, A. (2007). “Behavior of Flexural Strengthened Beams with
448 Prestressed CFRP Laminates.” *FRPRCS-8*, Patras, Greece.

449 ISO-527-2. *Plastics - Determination of tensile properties - Part 2: Test conditions*
450 *for moulding and extrusion plastics.*

451 ISO-527-5. *Plastics - Determination of tensile properties - Part 5: Test conditions*
452 *for unidirectional fibre-reinforced plastics.*

453 Kim, Y., Wight, R., and Green, M. (2008). “Flexural Strengthening of RC Beams
454 with Prestressed CFRP sheets: Development of nonmetallic anchor systems.”
455 *Journal of Composites for Construction*, 12(1), 35–43.

456 Kotynia, R., Walendziak, R., Stoecklin, I., and Meier, U. (2011). “RC Slabs strength-
457 ened with Prestressed and Gradually Anchored CFRP Strips under Monotonic and
458 Cyclic Loading.” *Journal of Composites for Construction*, 15(2), 168–180.

459 Meier, U. and Stöcklin, I. (2005). “A Novel Carbon Fiber reinforced Polymer (CFRP)
460 System for Post-Strengthening.” *International Conference on Concrete Repair,*
461 *Rehabilitation and Retrofitting (ICCRRR)*, Cape Town, South Africa.

462 Michels, J., Czaderski, C., Brönnimann, R., and Motavalli, M. (2012a). “Gradi-
463 ent Anchorage method for Prestressed CFRP Strips - Principle and Application.”
464 *Bridge Maintenance, Safety, Management, Resilience and Sustainability - Pro-*
465 *ceedings of the Sixth International Conference on Bridge Maintenance, Safety and*
466 *Management*, Stresa, Italy, 1981–1986.

467 Michels, J., Czaderski, C., El-Hacha, R., Brönnimann, R., and Motavalli, M. (2012b).
468 “Temporary Bond Strength of Partly Cured Epoxy Adhesive for Anchoring Pre-

469 stressed CFRP Strips on Concrete.” *Composite Structures*, 94(9), 2667–2676.

470 Motavalli, M., Czaderski, C., and Pfyl-Lang, K. (2011). “Prestressed CFRP for
471 Strengthening of Reinforced Concrete Structures: Recent developments at empa,
472 switzerland.” *Journal of Composites for Construction*, 15(2), 194–205.

473 Neubauer, U., Vom Berg, W., and Onken, P. (2007). “Structural Strengthening with
474 a new System of Prestressed CFRP Strips.” *FRPRCS-8*, Patras, Greece.

475 Pellegrino, C. and Modena, C. (2009). “Flexural Strengthening of real-scale RC and
476 PRC Beams with End-anchored Pretensioned FRP Laminates.” *ACI Structural
477 Journal*, 106(3), 319–328.

478 S&P-Clever-Reinforcement-Company-AG (2011). *Qualitätsprüfzeugnis 052641 IG
479 CFK 150/2000 S100/1.2 / Charge:706032*. S&P Clever Reinforcement Company
480 AG.

481 S&P-Clever-Reinforcement-Company-AG (2012). *S&P Resin 220 epoxy adhesive -
482 Technical data sheet*. S&P Clever Reinforcement Company AG.

483 Stöcklin, I. and Meier, U. (2001). “Strengthening of Concrete Structures with Pre-
484 stressed and Gradually Anchored CFRP Strips.” *FRPRCS-5*, Cambridge, UK.

485 Suter, R. and Jungo, D. (2001). “Vorgespannte CFK-Lamellen zur Verstärkung von
486 Bauwerken.” *Beton- und Stahlbetonbau*, 96(5), 350–358.

487 Svecova, D. and Razaqpur, A. (2000). “Flexural Behavior of Concrete Beams rein-
488 forced with Carbon Fiber-Reinforced Polymer CFRP Prestressed Prisms.” *ACI
489 Structural Journal*, 97(5), 731–738.

490 Tateishi, A., Kobayashi, A., Sato, S., and Yasumori, H. (2007). “An Experimental
491 Study on Tensioned CFRP Strip Method with Deviator.” *FRPRCS-8*, Patras,

492 Greece.

493 Triantafillou, T. C., Deskovic, N., and Deuring, M. (1992). “Strengthening of Con-
494 crete Structures with Prestressed Fiber Reinforced Plastic Sheets.” *ACI Structural*
495 *Journal*, 89(3), 235–244.

496 Wight, R., Green, M., and Erki, M.-A. (2001). “Prestressed FRP Sheets for Post-
497 strengthening Reinforced Concrete Beams.” *Journal of Composites for Construc-*
498 *tion*, 5(4), 214–220.

499 Woo, S.-K., Nam, J.-W., Kim, J.-H., Han, S.-H., and Byun, K. (2008). “Suggestion of
500 Flexural Capacity Evaluation and Prediction of Prestressed CFRP Strengthened
501 Design.” *Engineering Structures*, 30(12), 3751–3763.

502 Wu, Z., Iwashita, K., Hayashi, K., Higuchi, T., Murakami, S., and Koseki, Y.
503 (2003). “Strengthening Prestressed-concrete Girders with Externally Prestressed
504 PBO Fiber Reinforced Polymer Sheets.” *Journal of Reinforced Plastics and Com-*
505 *posites*, 22(14), 1269–1286.

506 Xue, W., Tan, Y., and Zeng, L. (2010). “Flexural Response Predictions of Rein-
507 forced Concrete Beams Strengthened with Prestressed CFRP Plates.” *Composite*
508 *Structures*, 92(3), 612–622.

509 Xue, W., Zeng, L., and Tan, Y. (2008). “Experimental Studies on Bond Behaviour
510 of High Strength CFRP Plates.” *Composites Part B: Engineering*, 39(4), 592–603.

511 **List of Tables**

512 1 Average results of the unidirectional tensile tests on CFRP strip spec-
513 imens after different stress and heating conditions (CFRP-REF: un-
514 stressed, CFRP-PRE: prestressed, CFRP-PH: prestressed and heated) 25
515 2 Physical and mechanical characteristics of the S&P Resin 220 epoxy
516 resin according to the producer’s data sheet S&P Clever Reinforcement 26
517 3 Elastic modulus E_a and tensile strength $f_{a,u}$ of the epoxy specimens
518 cured at high temperature (HT, 90°C) for 25 minutes and cured at
519 room temperature (RT, 22°C) for 3 days 27
520 4 Summary of static beam tests (*estimated according to fib-bulletin 1) 28

TABLE 1: Average results of the unidirectional tensile tests on CFRP strip specimens after different stress and heating conditions (CFRP-REF: unstressed, CFRP-PRE: prestressed, CFRP-PH: prestressed and heated)

<i>Specimen</i>		b_f [mm]	t_f [mm]	F_{max} [kN]	$f_{f,u}$ [MPa]	E_f [GPa]
CFRP-REF	X_{min}	15.1	1.2	44.8	2548.7	157.6
	X_m	15.1	1.2	49.1	2761.2	162.0
	X_{max}	15.1	1.2	54.0	3007.5	167.8
	CoV	0.1%	0.7%	7.6%	6.9%	3.2%
CFRP-PRE	X_{min}	15.1	1.2	45.3	2572.3	158.9
	X_m	15.1	1.2	48.2	2707.6	163.6
	X_{max}	15.1	1.2	51.2	2901.0	169.4
	CoV	0.1%	0.7%	5.2%	5.4%	2.5%
CFRP-PH	X_{min}	15.1	1.2	44.9	2427.3	150.4
	X_m	15.2	1.2	48.0	2632.2	161.2
	X_{max}	15.2	1.2	51.5	2889.5	166.6
	CoV	0.3%	1.4%	4.7%	6.0%	3.5%

TABLE 2: Physical and mechanical characteristics of the S&P Resin 220 epoxy resin according to the producer's data sheet S&P Clever Reinforcement

<i>Property</i>	<i>Value</i>
Components	A (resin) and B (hardener)
Color	Light grey Component A
	Black Component B
	Light grey Final mix (A+B)
Mixing ratio	4 : 1 (A : B) by weight or volume
Glass transition temperature	$\geq 56^{\circ}\text{C}$
Pot life	≥ 60 min. at $+20^{\circ}\text{C}$
Bending tensile strength	≥ 30 MPa
Compression strength	≥ 90 MPa
Adhesive strength	≥ 3 MPa (on concrete and on S&P laminates)

TABLE 3: Elastic modulus E_a and tensile strength $f_{a,u}$ of the epoxy specimens cured at high temperature (HT, 90°C) for 25 minutes and cured at room temperature (RT, 22°C) for 3 days

<i>Specimen</i>	<i>HT curing</i> E_a [GPa]	<i>RT curing</i> E_a [GPa]	<i>HT curing</i> $f_{a,u}$ [MPa]	<i>RT curing</i> $f_{a,u}$ [MPa]
1	5.9	6.9	11.8	21.9
2	5.7	(*)	16.1	(**)
3	5.2	7.9	12.5	20.6
4	4.3	7.9	13.2	21.5
5	4.0	7.9	9.5	19.0
6	3.7	7.8	8.8	19.9
X_{min}	3.7	6.9	8.8	19.0
X_m	4.8	7.7	12.0	20.6
X_{max}	5.9	7.9	16.1	21.9
CoV	15.6%	5.4%	16.5%	5.5%

TABLE 4: Summary of static beam tests (*estimated according to fib-bulletin 1)

Beam	$f_{cm,cube,28}$ [MPa]	$f_{c,cube,testing}$ [MPa]	$\varepsilon_{f,p}$ [%]	$4 \cdot F_{tot}$ [kN]	w_u [mm]	$\varepsilon_{f,u}$ [%]	$\Delta\varepsilon_f$ [%]
1	56.8	63.2	0.59	~80	127.4	1.42	0.83
2	54.3	57.7	0.59	69.9	91.2	1.16	0.57
3	52.2	54.0	0.60	80.9	125.3	1.38	0.78
4	54.1	69.4*	0.61	70.5	98.8	1.28	0.67

521 **List of Figures**

522 1 Schematic representation of the gradient anchorage 31

523 2 Force transfer in the different gradient segments 32

524 3 Different components of the anchorage device: a) base angles, b)

525 clamps, c) aluminum frame, d) manometer and valves, e) hydraulic

526 jack and f) electronic heating device 33

527 4 Installation procedure for the gradient anchorage devices 34

528 5 Cross section of the strengthened RC beam (dimensions in [mm]) . . 35

529 6 Plate bottom side during the strengthening application 36

530 7 Heating and force release configuration for the strengthening applica-

531 tion, a) Side view, b) Top view 37

532 8 a) Jack force F and CFRP strain $\varepsilon_{f,p}$ (outside the gradient area)

533 evolution over time t , and b) Temperature evolution over time t in the

534 heating elements $T_{h,j}$ and in the adhesive $T_{a,k}$ 38

535 9 CFRP tensile strain ε_f evolution over time after anchoring 39

536 10 Specimen dimensions (in [mm]) and test configuration for the CFRP

537 tensile tests 40

538 11 SEM images of CFRP samples: a) REF - reference, b) PRE - pre-

539 stressed ($\sigma_p=1'000$ MPa) and c) PH - prestressed ($\sigma_p =1'000$ MPa)

540 and heated ($T_a \approx 90^\circ\text{C}$) 41

541 12 Specimen dimensions (in [mm]) and test configuration for the epoxy

542 resin tensile tests 42

543	13	Stress-strain curves from the uniaxial tensile tests on epoxy specimens	
544		- RT cured for 3 days and accelerated curing for 25 minutes at 90°C .	43
545	14	Loading and measurement scheme for static beam loading (SG=strain	
546		gauge)	44
547	15	Force-midspan deflection curve (no influence of dead-load measured)	
548		of the static loading tests (no force measurements available for Beam 1)	45
549	16	Prestressed CFRP strip anchored with the gradient anchorage applied	
550		on a concrete slab and stored in the laboratory. Long-term measure-	
551		ment results of the CFRP strip strains by a mechanical strain gauge	
552		since the year 2000	46

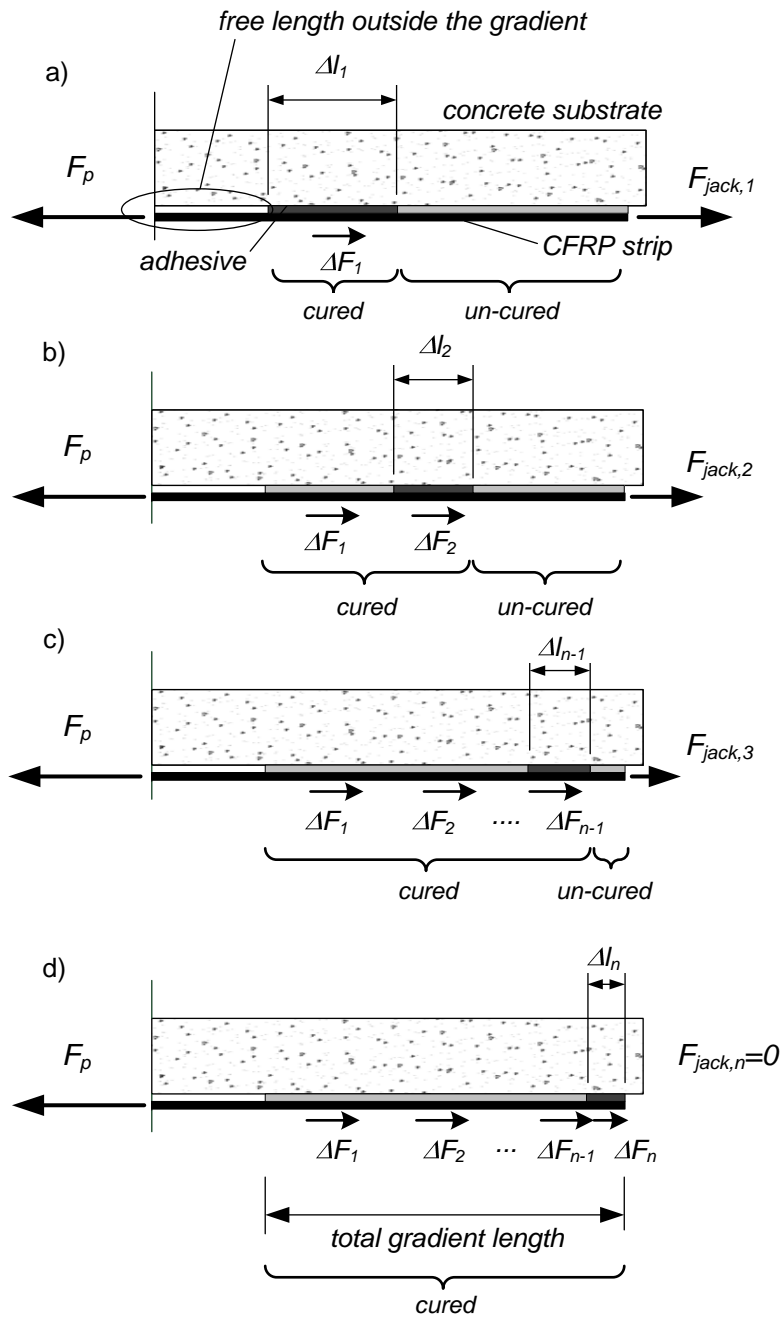


FIG. 1: Schematic representation of the gradient anchorage

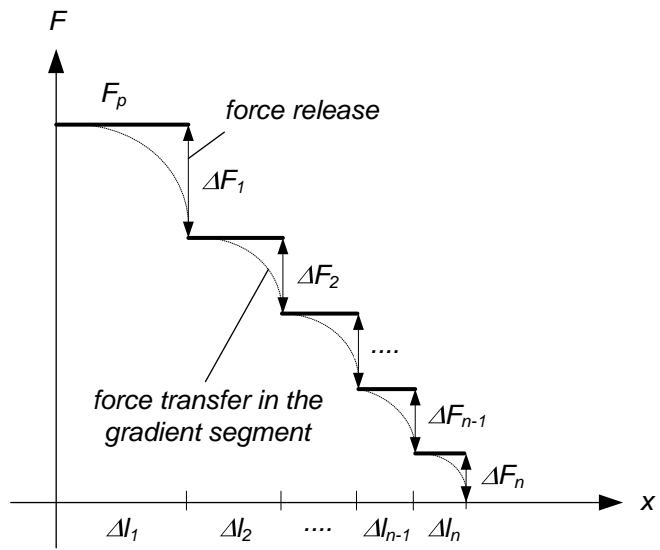


FIG. 2: Force transfer in the different gradient segments

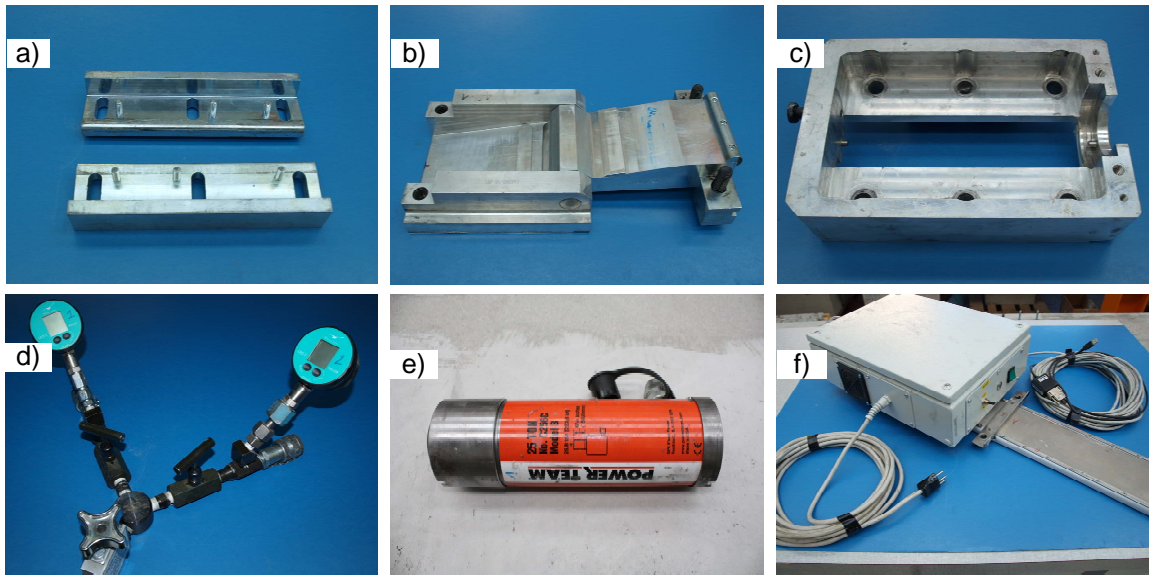


FIG. 3: Different components of the anchorage device: a) base angles, b) clamps, c) aluminum frame, d) manometer and valves, e) hydraulic jack and f) electronic heating device

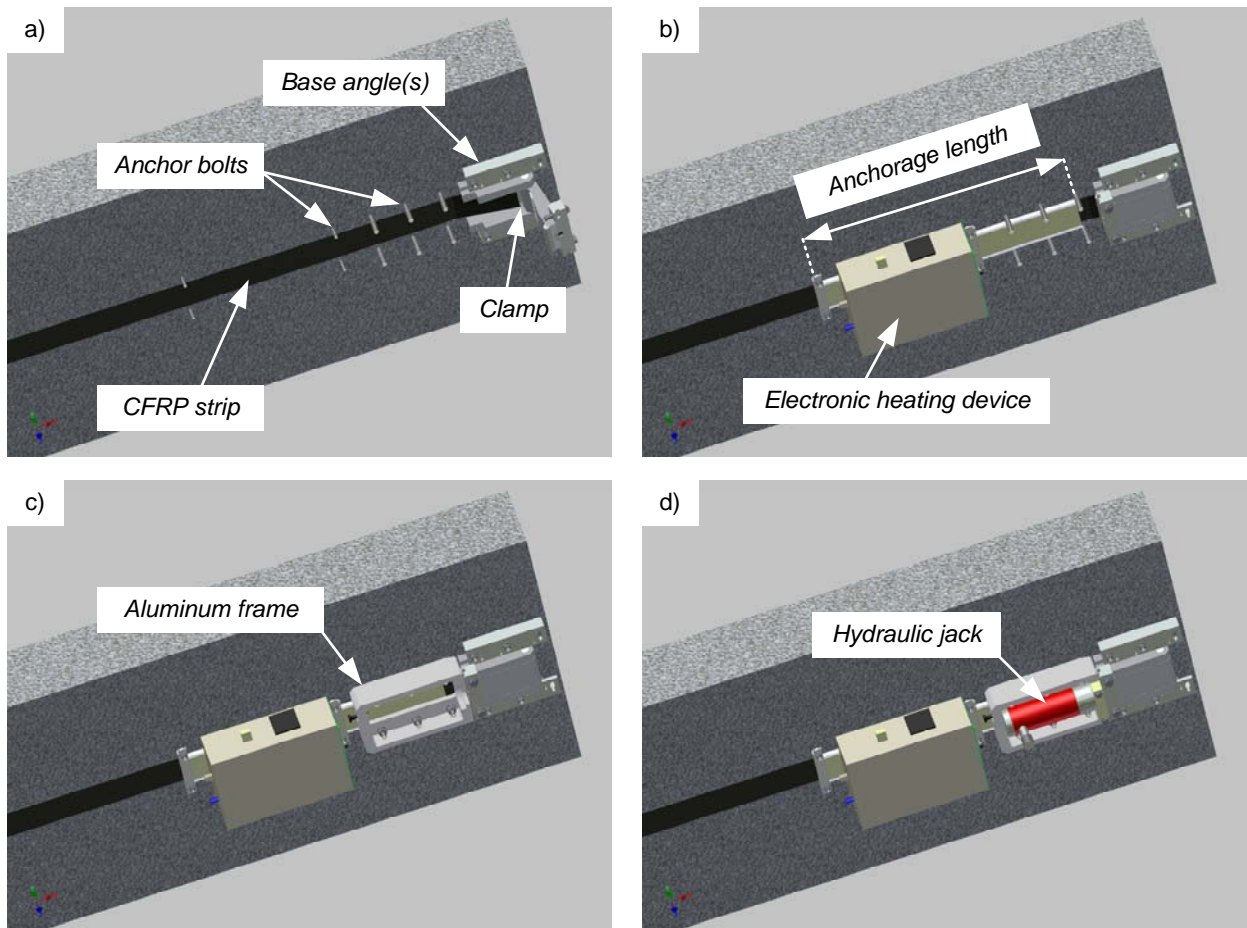


FIG. 4: Installation procedure for the gradient anchorage devices

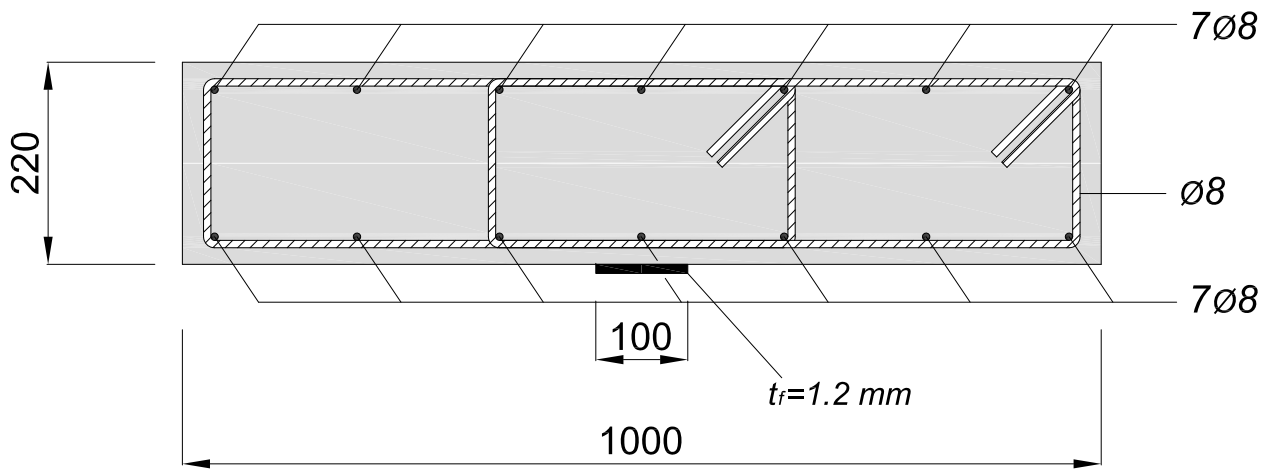


FIG. 5: Cross section of the strengthened RC beam (dimensions in [mm])

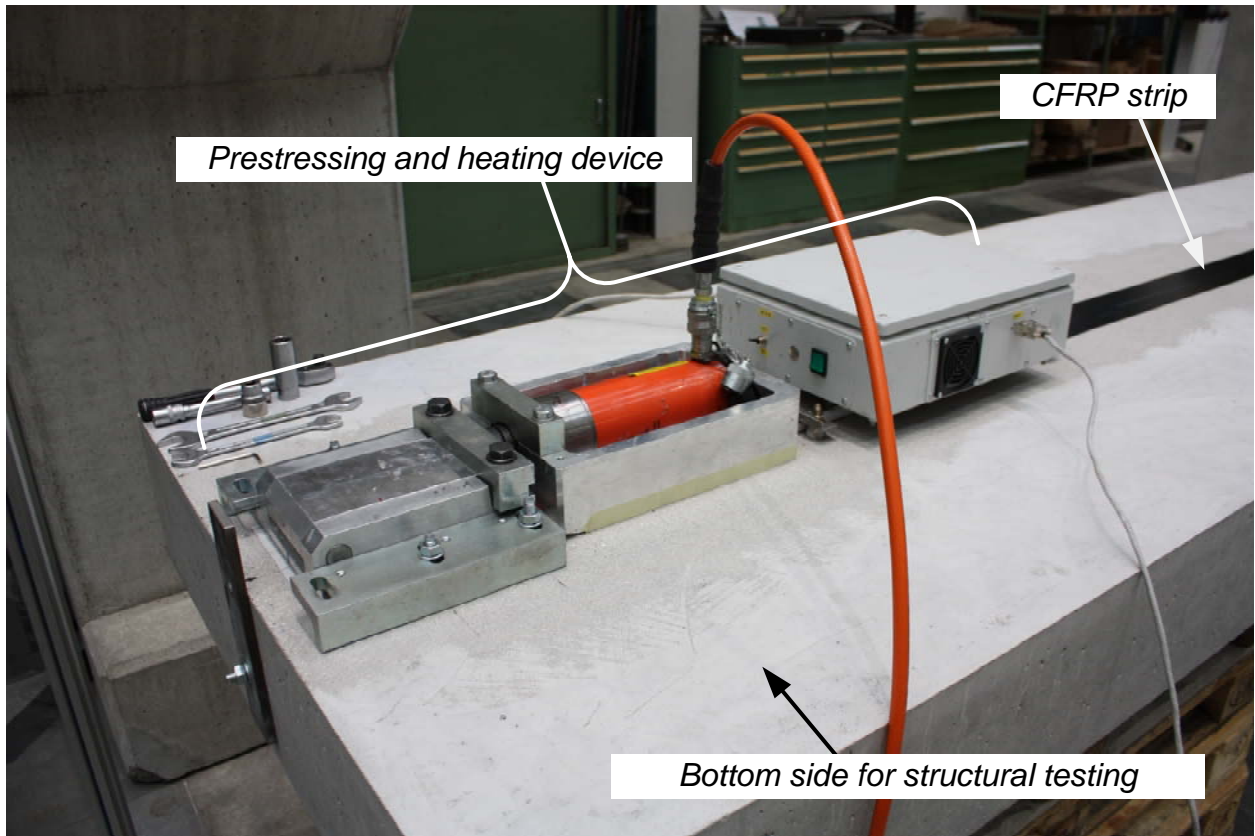


FIG. 6: Plate bottom side during the strengthening application

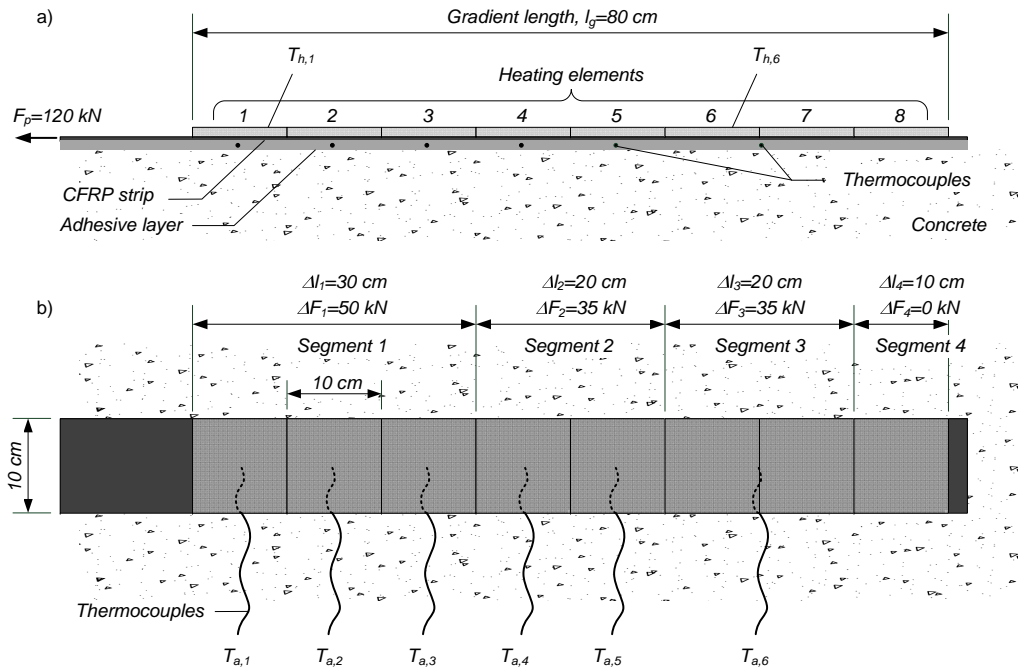


FIG. 7: Heating and force release configuration for the strengthening application, a) Side view, b) Top view

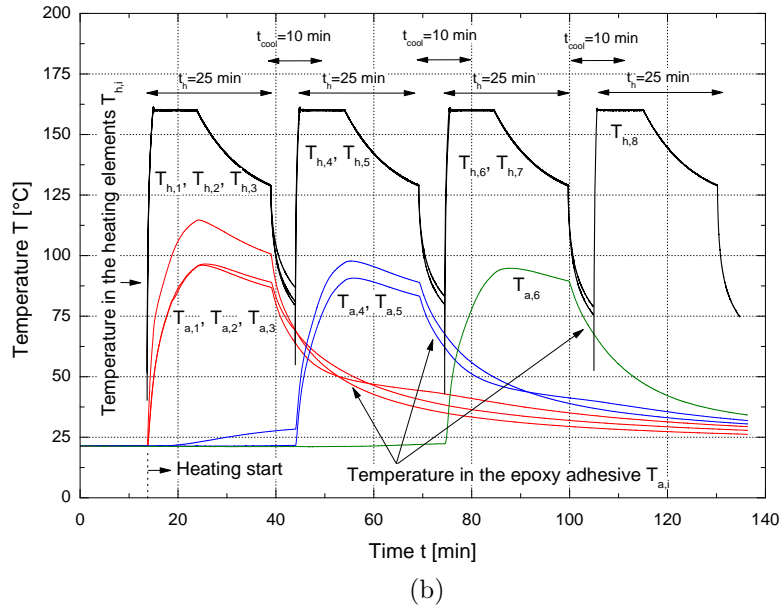
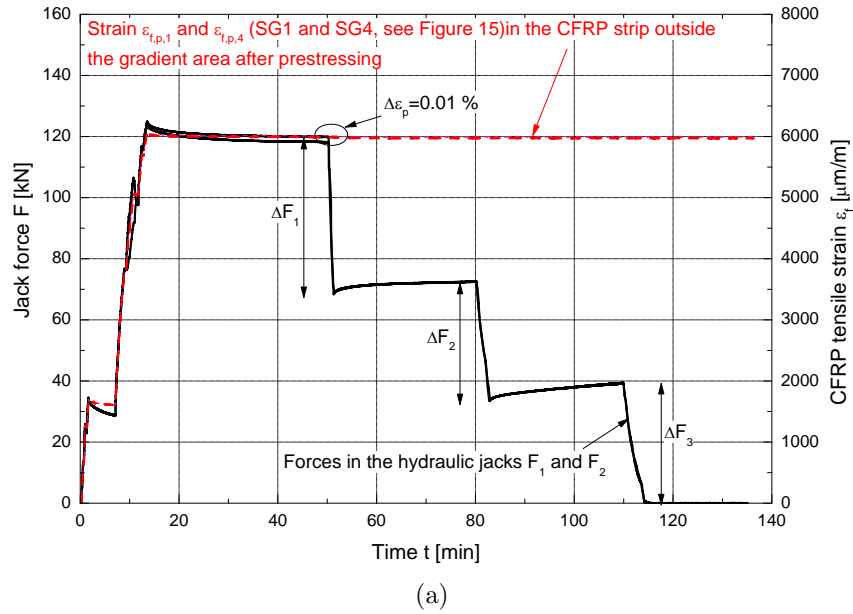


FIG. 8: a) Jack force F and CFRP strain $\varepsilon_{f,p}$ (outside the gradient area) evolution over time t , and b) Temperature evolution over time t in the heating elements $T_{h,j}$ and in the adhesive $T_{a,k}$

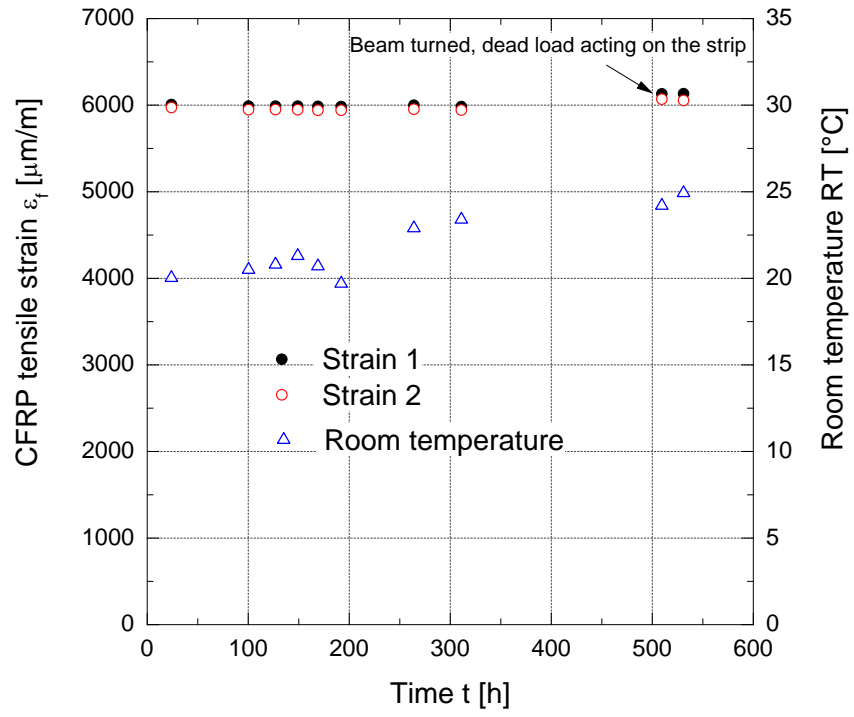


FIG. 9: CFRP tensile strain ε_f evolution over time after anchoring

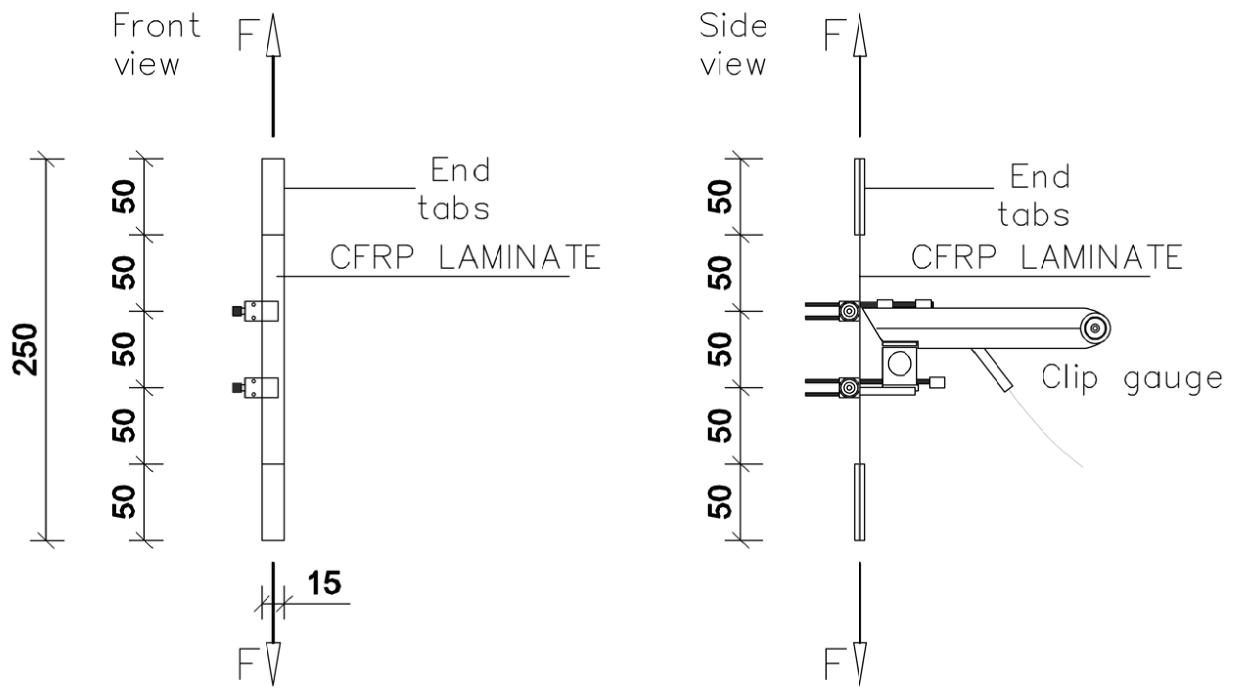


FIG. 10: Specimen dimensions (in [mm]) and test configuration for the CFRP tensile tests

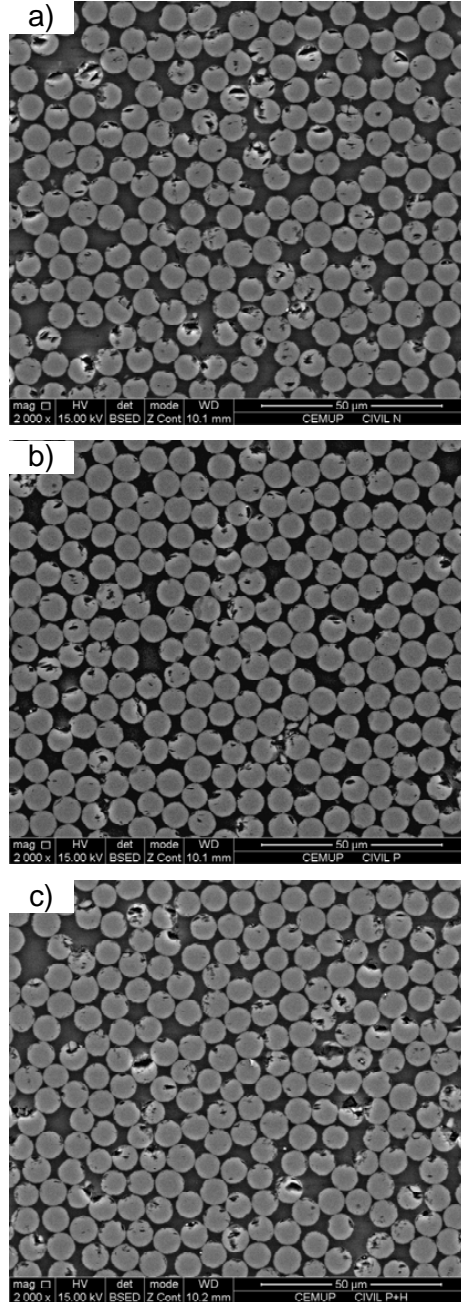


FIG. 11: SEM images of CFRP samples: a) REF - reference, b) PRE - prestressed ($\sigma_p=1'000$ MPa) and c) PH - prestressed ($\sigma_p=1'000$ MPa) and heated ($T_a \approx 90^\circ\text{C}$)

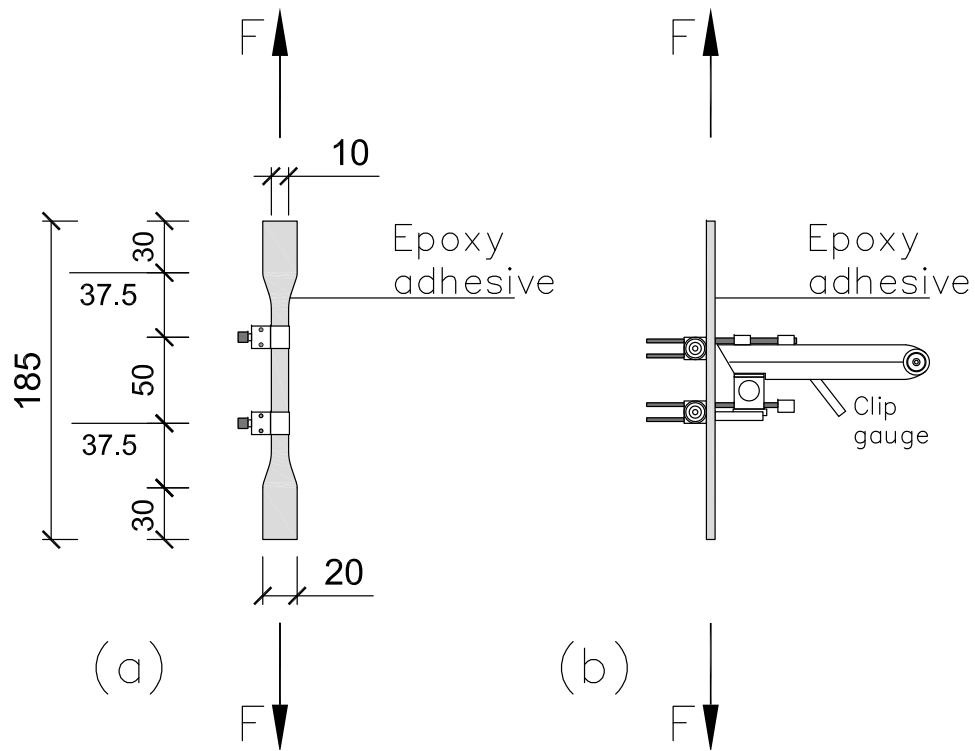


FIG. 12: Specimen dimensions (in [mm]) and test configuration for the epoxy resin tensile tests

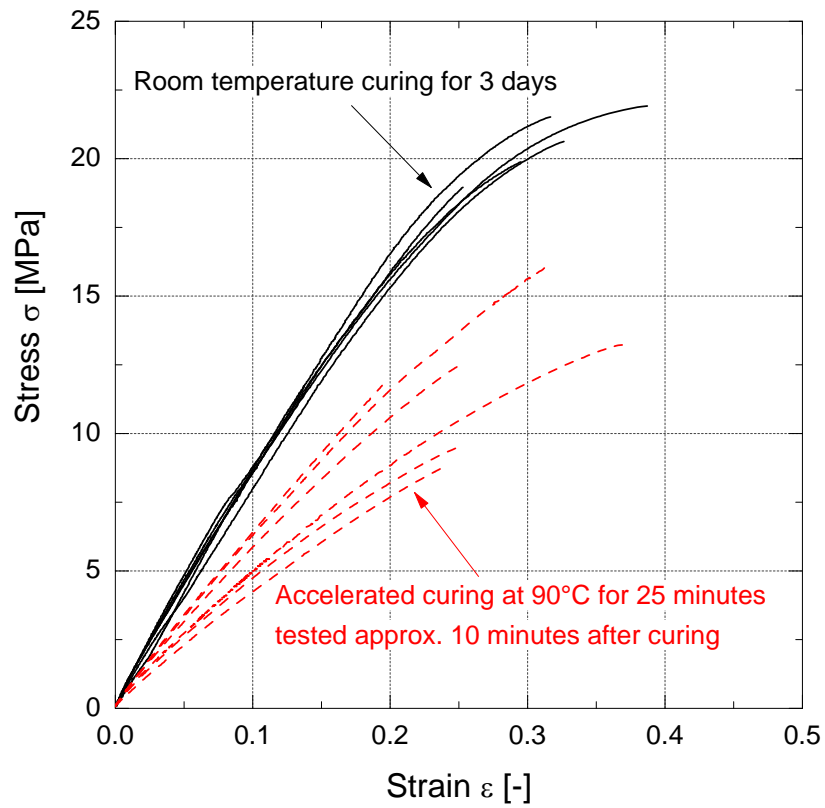


FIG. 13: Stress-strain curves from the uniaxial tensile tests on epoxy specimens - RT cured for 3 days and accelerated curing for 25 minutes at 90°C

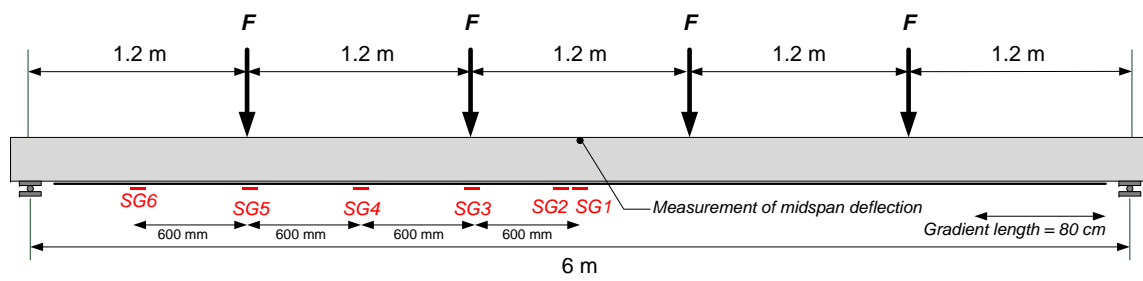


FIG. 14: Loading and measurement scheme for static beam loading (SG=strain gauge)

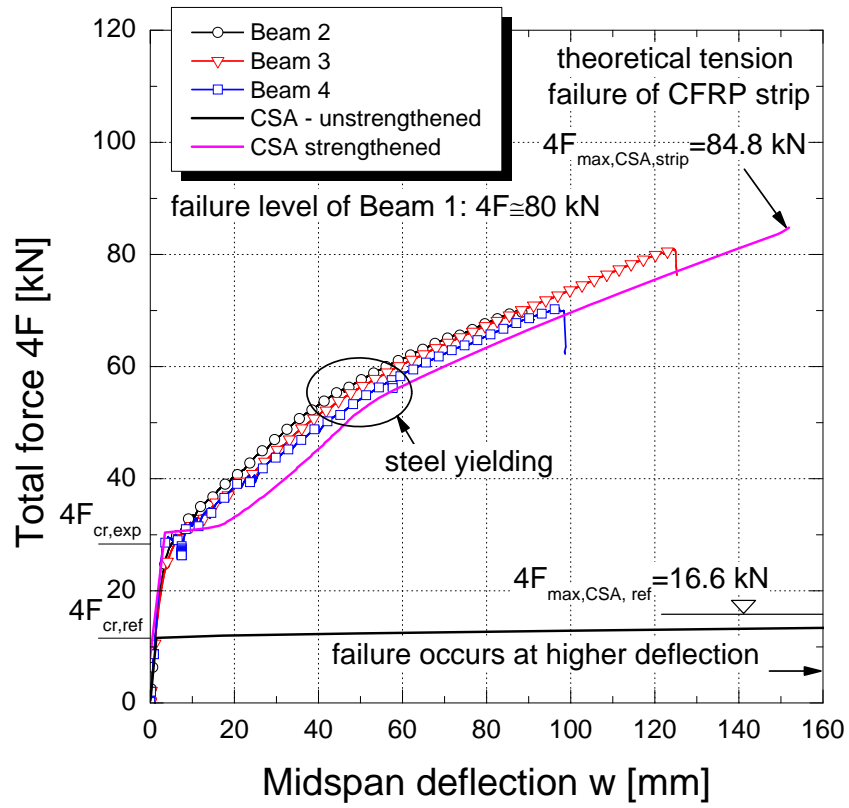


FIG. 15: Force-midspan deflection curve (no influence of dead-load measured) of the static loading tests (no force measurements available for Beam 1)

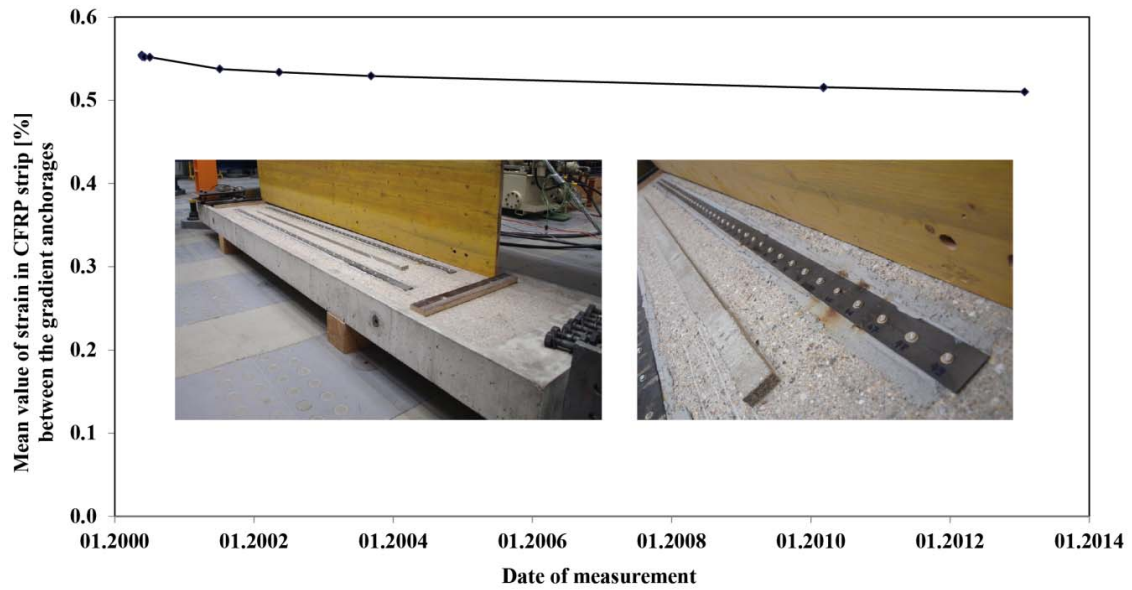


FIG. 16: Prestressed CFRP strip anchored with the gradient anchorage applied on a concrete slab and stored in the laboratory. Long-term measurement results of the CFRP strip strains by a mechanical strain gauge since the year 2000